Agriculture, Ecosystems and Environment 167 (2013) 33–37

Contents lists available at SciVerse ScienceDirect

Agriculture, Ecosystems and Environment

journal homepage: www.elsevier.com/locate/agee

Short communication

# Quantification of uncertainties associated with space-time estimates of short-term soil $CO_2$ emissions in a sugar cane area

D.D.B. Teixeira[a,*], E.S. Bicalho[a,b], C.E.P. Cerri[b], A.R. Panosso[a], G.T. Pereira[a], N. La Scala[a]

[a] Universidade Estadual Paulista, Departamento de Ciências Exatas – FCAV/UNESP, Via de Acesso Prof. Paulo Donato Castellane s/n, 14884-900 Jaboticabal, SP, Brazil
[b] Universidade de São Paulo, Departamento de Ciência do Solo – ESALQ/USP, Av. Páduas Dias, 11, CP. 9, 13418-900 Piracicaba, SP, Brazil

ARTICLE INFO

*Article history:*
Received 19 April 2012
Received in revised form 9 October 2012
Accepted 15 January 2013
Available online 1 March 2013

*Keywords:*
Soil respiration
Geostatistics
Sequential Gaussian simulation
Joint probability

ABSTRACT

The characterization of soil $CO_2$ emissions ($FCO_2$) is important for the study of the global carbon cycle. This phenomenon presents great variability in space and time, a characteristic that makes attempts at modeling and forecasting $FCO_2$ challenging. Although spatial estimates have been performed in several studies, the association of these estimates with the uncertainties inherent in the estimation procedures is not considered. This study aimed to evaluate the local, spatial, local-temporal and spatial-temporal uncertainties of short-term $FCO_2$ after harvest period in a sugar cane area. The $FCO_2$ was featured in a sampling grid of 60 m × 60 m containing 127 points with minimum separation distances from 0.5 to 10 m between points. The $FCO_2$ was evaluated 7 times within a total period of 10 days. The variability of $FCO_2$ was described by descriptive statistics and variogram modeling. To calculate the uncertainties, 300 realizations made by sequential Gaussian simulation were considered. Local uncertainties were evaluated using the probability values exceeding certain critical thresholds, while the spatial uncertainties considering the probability of regions with high probability values together exceed the adopted limits. Using the daily uncertainties, the local-spatial and spatial-temporal uncertainty (Ftemp) was obtained. The daily and mean emissions showed a variability structure that was described by spherical and Gaussian models. The differences between the daily maps were related to variations in the magnitude of $FCO_2$, covering mean values ranging from $1.28 \pm 0.11\ \mu mol\ m^{-2}\ s^{-1}$ (F197) to $1.82 \pm 0.07\ \mu mol\ m^{-2}\ s^{-1}$ (F195). The Ftemp showed low spatial uncertainty coupled with high local uncertainty estimates. The average emission showed great spatial uncertainty of the simulated values. The evaluation of uncertainties associated with the knowledge of temporal and spatial variability is an important tool for understanding many phenomena over time, such as the quantification of greenhouse gases or the identification of areas with high crop productivity.



## 1. Introduction

Human actions related to land management can interfere with the flow of carbon between terrestrial ecosystems and the atmosphere (Morell et al., 2010; Sugihara et al., 2012). It is estimated that in 2005, agriculture was responsible for an emission of 5.1–6.1 Gt of $CO_2$ eq year$^{-1}$, corresponding to approximately 10% to 12% of the total anthropogenic emissions of greenhouse gases (IPCC, 2007). Soil $CO_2$ emissions ($FCO_2$) combined with erosion processes are the main sources of soil carbon loss (Mchunu and Chaplot, 2012), although erosion may also contribute to the significant increase in soil carbon stocks (Boix-Fayos et al., 2009).

The $FCO_2$, as well as other soil properties, presents a complex degree of variability in space (Panosso et al., 2009; Herbst et al., 2010; Prolingheuer et al., 2010; Teixeira et al., 2011, 2012; Jurasinski et al., 2012) and time (Herbst et al., 2009; Iqbal et al., 2010; Luan et al., 2012) showing a great variability even in short periods (La Scala et al., 2000; Teixeira et al., 2011). Such variability is a combination of several biological, chemical and physical interactions acting at multiple scales (Parkin, 1993). Tools such as geostatistics have been used for providing the capture, representation and interpretation of the spatial patterns of this variable.

During the process of interpolation of unsampled sites, it is possible to identify some imprecision sources of the estimates, which are evaluated by quantifying the errors and uncertainties of non-sampled locations. Errors are defined as the difference between the calculated value and the real value of a property at the same location in space (Isaaks and Srivastava, 1989). On the other hand, uncertainties correspond to the doubt in estimated value which cannot be compared to the real value, since this is not available. Thus, here it is considered that cross-validation and

* Corresponding author. Tel.: +55 16 3209 2625.
*E-mail addresses:* daniel.dbt@hotmail.com, danieldbt@bol.com.br (D.D.B. Teixeira), eltonbicalho@ig.com.br (E.S. Bicalho), cepcerri@usp.br (C.E.P. Cerri), arpanosso@yahoo.com.br (A.R. Panosso), genertp@fcav.com.br (G.T. Pereira), lascala@fcav.unesp.br (N. La Scala).

0167-8809/$ – see front matter © 2013 Elsevier B.V. All rights reserved.
http://dx.doi.org/10.1016/j.agee.2013.01.004

external-validation analysis (see Deutsch and Journel, 1998) are able to provide errors while the cumulative distribution functions (cdf) provide the uncertainty of the studied phenomena.

Several interpolation techniques can be used to generate maps of estimated soil properties. Ordinary kriging (OK), indicator kriging (IK) and sequential Gaussian simulation (SGS) are the main geostatistical interpolations used. Kriging estimators provide the best estimate of the local variables by minimizing the variance estimate, resulting in smoothing of the spatial details. The use of the kriging variance as a local error measure is inappropriate when the data configuration together with the uncertainty in the estimates are considered (Zhao et al., 2009) because only the variogram and the sample configuration are considered in its calculations. As with other analyses, except if a Gaussian model is assumed for errors, kriging provides only an incomplete measure of location accuracy and no consideration of the joint accuracy can be made when several locations are considered together (Deutsch and Journel, 1998). Techniques such as IK only evaluate the uncertainty location and are unable to detect the spatial uncertainties associated with estimates. Such uncertainties are based only on the spatial variation of the known values, without considering the variation in estimates of non-sampled locations (Delbari et al., 2009). Goovaerts (2001) stated that the cdf obtained by IK only provide a measure of local uncertainty and that no quantitative measure of the spatial uncertainty is obtained.

These simulation methods are used in situations where reproducing spatial variability, honoring the inferred heterogeneity in the data, and assessing the impact of uncertainties are required (Goovaerts, 1999). The simulations are stochastic processes of design alternatives that are equally probable joint realizations of a component of a random variable from the model of a random function (Deutsch and Journel, 1998). Simulations have recently started to be adopted for the evaluation of $FCO_2$ in agricultural soils (Herbst et al., 2010; Teixeira et al., 2011, 2012), with the aim of improving the quality of the interpolations obtained. In this context, the objective of this paper is to characterize the local, spatial and spatio-temporal uncertainties of $FCO_2$ estimates at the mesoscopic scale (area of 0.36 ha) over 10 days of evaluation (short period) through many equiprobable realizations of the SGS.

## 2. Materials and methods

The study was conducted in Guariba in São Paulo State (21°21′S, 48°11′W). According to the Thornthwaite classification, the local climate can be defined as B1rB′4a′-type mesothermal humid, with little water stress, evapotranspiration and less than 48% annual evapotranspiration in the summer. The soil of the area was classified as a high clay Oxisol.

The area has been cultivated with sugar cane (*Saccharum* spp. var. SP86-155) for 8 years under a management system using mechanical harvesting. At the time of the study, the soil was devoid of vegetation and was covered with large amounts of crop residue (12 t $ha^{-1}$) from mechanical harvesting performed a few days before the start of the experiment. On July 13th, 2010, a regular grid of 60 m × 60 m was installed containing 127 points spaced at minimum distances of 0.5–10 m from the installation of PVC collars, which were used to assess the $FCO_2$.

The $FCO_2$ was assessed using three portable systems (LI-COR 8100). The soil chambers are coupled to a system that quantifies the internal concentration of $CO_2$ through optical absorption spectroscopy in the infrared spectral region. Before starting the experiment, the machines were tested and calibrated. The

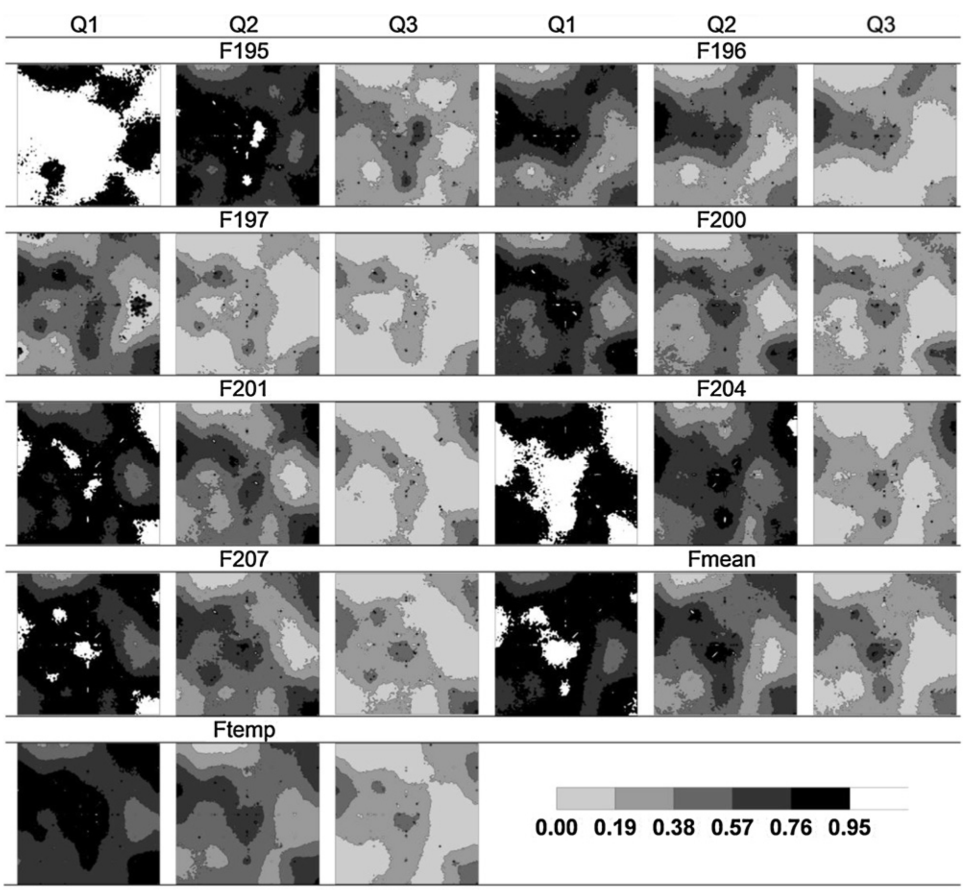


**Fig. 1.** Probability maps of the values estimated exceeding the values of the quartiles (Q1, Q2, Q3). F___ = days of the year that soil $CO_2$ emission was evaluated.

evaluations were conducted in the morning (8:00–9:30 am) over 7 days on Julian days 195 (F195), 196 (F196), 197 (F197), 200 (F200), 201 (F201), 204 (F204) and 207 (F207) in 2010. After the readings were calculated, the average emission (Fmean) considering the values observed in the different days was evaluated.

The short period (10 days) stands out as the period that the $FCO_2$ is more related to the soil organic carbon losses (Cerri et al., 2011), once the soil is almost bare having few vegetation (Panosso et al., 2009). This post-harvest period also focus the impact of the main agricultural operations due to the harvest and other management practices which contribute largely to the increased rates of soil respiration. As sugar cane is a crop with rapid vegetative growth, the quantification of soil respiration coming mostly from the soil over longer periods is difficult. Moreover, due to the intense root growth, autotrophic respiration quickly integrates the captured emissions from the soil. Thus studies of temporal variations of $FCO_2$, obtained directly, are commonly evaluated for short periods after harvest or tillage operations (La Scala et al., 2000; Brito et al., 2010; Panosso et al., 2011).

The $FCO_2$ variability was described initially by using descriptive statistics and then using the geostatistical modeling of the experimental variogram based on the principles of the intrinsic hypothesis (Deutsch and Journel, 1998) (Eq. (1)).

$$\hat{\gamma}(h) = \frac{1}{2N(h)} \sum_{i=1}^{N(h)} [z(x_i) - z(x_i + h)]^2 \quad (1)$$

where $\hat{\gamma}(h)$ is the experimental semivariance a separation distance $h$, $z(x_i)$ is the property value of $FCO_2$ at the $i$th point, and $N(h)$ is the number of pairs of points separated by distance $h$. The choice of the variogram model is adjusted based on the residual sum of squared (RSS) and the coefficient of determination ($R^2$).

After modeling, 300 realizations of SGS were made in accordance with the SGSIM-routine of the Geostatistical Software Library (Deutsch and Journel, 1998). The SGS allows the quantification of local and spatial uncertainties related to simulated values in unsampled locations. Local daily uncertainty was previously evaluated by calculating the probability of the point values exceeding a certain critical limit (Delbari et al., 2009; Zhao et al., 2009). The limits used in this study were 0.79, 1.31 and 1.95 $\mu$mol m$^{-2}$ s$^{-1}$, representing the 1st (Q1), 2nd (Q2) and 3rd (Q3) quartiles of the variable Fmean, respectively. This procedure quantifies the number of simulated maps in which the variable occasionally exceeds the limit indicated (Eq. (2)).

$$\text{Prob}[z(x_0) \geq z_c] = \frac{n(x_0)}{L} \quad (2)$$

where $z(x_0)$ is the value of the variable $z$ in the location $x_0$, $z_c$ is the critical limit adopted, $n(x_0)$ is the number of realizations to which the variable displays a value above $z_c$ and $L$ is the total number of realizations generated. In this study, $L$ = 300 for average and daily emissions.

To supplement the location uncertainty, the spatial uncertainty was evaluated based on the calculation of the joint probability (Pj) (Juang et al., 2004). The Pj helps determine the reliability of the areas outlined with a high probability that the simulated values exceed the critical limits (Prob[$z(x_0) \geq z_c$]). To calculate the Pj, areas that had a probability greater than or equal to 95%, calculated based on Eq. (2), were considered. The procedure consists of counting the number of realizations in which all locations (with probability greater than or equal to 95%) simultaneously appear above the critical value.

$$\text{Prob}[z(x_{01}) \geq z_c, z(x_{02}) \geq z_c, \ldots, z(x_{0N}) \geq z_c] = \frac{n(x_{01}, x_{02}, \ldots, x_{0N})}{L} \quad (3)$$

where $n(x_{01}, x_{02}, \ldots, x_{0n})$ is the number of realizations in which the simulated values at the locations $x_{01}, x_{02}, \ldots, x_{0n}$ have joint values above the critical limit adopted ($z_c$), and $L$ is the number of realizations made in the simulation ($L$ = 300). Values closer to 1 provide greater reliability and reduce the spatial uncertainty of the area.

The calculation of the local time uncertainty (Ftemp) and space-time were performed considering all maps produced daily. Thus, in Eqs. (2) and (3), $L$ = 2100 was used for Ftemp, accounting for all the realizations produced by the SGS on the 07 days evaluated.

## 3. Results and discussion

The temporal variability of $FCO_2$ throughout the evaluated day showed small variations, differing significantly ($p < 0.05$) between the emissions related to F195 (1.82 ± 0.07 $\mu$mol m$^{-2}$ s$^{-1}$) and F197 (1.28 ± 0.11 $\mu$mol m$^{-2}$ s$^{-1}$) by the Student's $t$ test (Table 1). This result may be related to homogeneous climatic conditions, with few variations in temperature and humidity over the short study period. The $FCO_2$ daily values were similar to those observed by Brito et al. (2010) in the same soil type and vegetation. Panosso et al. (2011), also in areas of sugar cane, observed average emission values of 2.07 ± 0.06 and 2.74 ± 0.14 $\mu$mol m$^{-2}$ s$^{-1}$ under green and slash-and-burn managements, respectively. The high CV values (>40%) indicate a high variability of the data, demonstrating the need for a more rigorous statistical analysis that enables the evaluation and interpretation of $FCO_2$ in different compartments of the area. These values are similar to those found by other authors in several soil and cultivation types (Herbst et al., 2009; Brito et al., 2009).

**Table 1**
Descriptive statistics and the variogram parameters fitted to the data of soil $CO_2$ emission ($\mu$mol m$^{-2}$ s$^{-1}$).

| | Mean | CV[a] | Model | $C_0$[b] | $C_0 + C_1$[c] | $A$[d] | $C_0/C_0 + C_1$[e] | $R^2$ | RSS[f] |
|---|---|---|---|---|---|---|---|---|---|
| F195 | 1.82 ± 0.07a | 41.70 | Sph.[g] | 0.62 | 1.10 | 34.23 | 0.56 | 0.95 | 1.07E−02 |
| F196 | 1.52 ± 0.12bc | 85.72 | Gaus.[h] | 0.58 | 1.19 | 33.43 | 0.48 | 0.94 | 2.88E−02 |
| F197 | 1.28 ± 0.11c | 93.04 | Sph. | 0.49 | 1.07 | 26.16 | 0.46 | 0.69 | 1.31E−01 |
| F200 | 1.53 ± 0.11bc | 74.29 | Sph. | 0.53 | 1.08 | 29.45 | 0.49 | 0.94 | 3.13E−02 |
| F201 | 1.49 ± 0.07bc | 49.16 | Sph. | 0.51 | 1.15 | 37.34 | 0.44 | 0.93 | 3.52E−02 |
| F204 | 1.63 ± 0.07b | 48.05 | Sph. | 0.51 | 1.27 | 46.32 | 0.40 | 0.80 | 1.74E−01 |
| F207 | 1.51 ± 0.07bc | 53.54 | Gaus. | 0.52 | 1.02 | 26.71 | 0.51 | 0.94 | 1.53E−02 |
| Fmean | 1.57 ± 0.07 | 50.02 | Gaus. | 0.68 | 1.19 | 25.39 | 0.57 | 0.90 | 3.70E−02 |

$N$ = 127; means followed by the same letters on a column do not differ (Student's $t$-test; $p \leq 0.05$).
[a] Coefficient of variation.
[b] Nugget effect.
[c] Sill.
[d] Range (m).
[e] Degree of spatial dependence.
[f] Residual sum of square.
[g] Spherical model.
[h] Gaussian model.

The Gaussian and spherical models were adjusted to the $FCO_2$ experimental variograms (Table 1). The Gaussian model describes phenomena with great continuity at small and large scales, while the spherical model, by presenting a well-defined sill, describes properties with abrupt changes along the ground (Deutsch and Journel, 1998). Brito et al. (2010) fitted spherical and exponential models to the $FCO_2$ data in different topographic positions in soils under cultivation of sugar cane. Teixeira et al. (2011) used spherical models to describe the diurnal spatial variability of $FCO_2$ in soils devoid of vegetation.

The use of normalized values for the construction of the variogram used in the process of SGS allows comparison of the effect nugget ($C_0$) between the daily variogram. The $C_0$ represents the combination of errors due to variability present on a smaller scale than that evaluated (in this case, less than 0.50 m) and those arising from laboratory determination methods. The Fmedio had the highest $C_0$ value (0.68) among the models, which was most likely due to its calculations based on average daily values, thus affecting the variability that is inherent in these data. Among the daily values, the higher $C_0$ was found for the largest daily emission (F195), and the lower $C_0$ was related to lower emissions (F197). This result indicates a larger error in the estimates of non-sampled locations on the days that $FCO_2$ has high emission values.

The range values ($A$) indicates the distance limit of spatial dependence between the samples; in other words, above this limit they are considered independently, showing no spatial relationship to each other. The range values varied from 25.39 (Fmean) to 46.32 m (F204), similar to values found by other studies (Brito et al., 2010; Teixeira et al., 2011). Prolingheuer et al. (2010) studied the spatial and temporal variability of soil respiration in areas under the cultivation of winter wheat, and they identified average range values of 18.0 m. Herbst et al. (2009), in a fine sampling grid of 14 m × 14 m, observed an average range of 2.7 m for $FCO_2$. These results are lower than those found in this study due to the extremely detailed level adopted by the authors. All models showed a moderate degree of spatial dependence, characterized by the relation $0.25 < C_0/C_0 + C_1 < 0.75$ (Cambardella et al., 1994).

Although the use of different realizations of the SGS allows a visual evaluation of the spatial uncertainties associated with estimates of the property values in question (Grunwald et al., 2007), quantification is possible only through the analysis of Pj (Table 2). Zhao et al. (2009), using the calculation of Pj, evaluated spatial area uncertainty with nutrient deficiency in soil. They observed small spatial uncertainties for organic matter and large uncertainties for the potassium and phosphorus content in the soil. Delbari et al. (2009) evaluated the reliability of areas susceptible to erosion using the same method.

**Table 2**
Evaluation of the spatial uncertainty of the areas that have values above the limits of 0.79 (Q1), 1.31 (Q2) and 1.95 (Q3) $\mu mol\ m^{-2}\ s^{-1}$.

| | Q1 | | Q2 | | Q3 | |
|---|---|---|---|---|---|---|
| | NSL[a] | Pj[b] | NSL | Pj | NSL | Pj |
| F195 | 5780 | 0.00 | 227 | 0.00 | 34 | 100.00 |
| F196 | 74 | 57.33 | 42 | 100.00 | 27 | 100.00 |
| F197 | 41 | 100.00 | 22 | 100.00 | 17 | 100.00 |
| F200 | 75 | 73.33 | 42 | 100.00 | 30 | 100.00 |
| F201 | 990 | 0.00 | 51 | 100.00 | 23 | 100.00 |
| F204 | 3623 | 0.00 | 131 | 31.33 | 25 | 100.00 |
| F207 | 738 | 0.00 | 48 | 100.00 | 26 | 100.00 |
| Fmean | 915 | 0.00 | 60 | 67.33 | 36 | 88.67 |
| Ftemp | 32 | 79.29 | 14 | 100.00 | 5 | 100.00 |

[a] Number of simulated locations.
[b] Joint probability (%).

Fig. 1 shows probability maps of emission values higher than those observed for the Fmean quartiles. The quartiles of the observed data were used in the absence of reference values for $FCO_2$ because few studies have promoted their characterization under the same type of soil and cultivation. The maps referring to the $Q1$ values generally have large areas with a high probability of exceeding this value. However, using $Q3$ as the limit, the maps do not exhibit continuous areas of high probability, being limited only to reproducing the values measured in the field (greater than $Q3$, with high probability) because no estimate is generated at these sites.

The difference between the maps of probability is related to daily variations in the magnitude of the emission, where days with higher average emissions (Table 1) have larger areas with a high probability of exceeding the limit used (Fig. 1). Overall, the largest emissions were located in the center and left center of the map, thus providing the greatest probability of having values above the critical limit adopted. The maps of the local temporal uncertainties (Ftemp) do not show continuous areas of high probability, a fact indicative of the great variation and low temporal persistence of $FCO_2$ even in the short study period (10-day), when no significant changes in the weather conditions, especially temperature and soil moisture, were observed.

Quantifying the spatial uncertainty by Pj shows that as the limit values increase, the area with the probability of showing values above these decreases, thus decreasing the number of simulated locations (NSL) (Table 2). With the exception of Fmean, in any variable values were simulated with a high probability of being larger than $Q3$, so only the punctual observations were considered in the calculations, resulting in Pj values equal to 100%. F195 and F204 had the highest spatial uncertainties, both with a 0.00% probability of exceeding $Q1$ and 0.00 and 31.33% probability of exceeding $Q2$, respectively. This greater uncertainty was due to a larger area of values above the simulated $Q1$ and $Q2$ limits (NSL value). The Fmean shows great spatial uncertainty even with small areas considered, while the Ftemp has low spatial uncertainty related to the high local uncertainty of the values simulated. Teixeira et al. (2011), evaluating the daily changes in $FCO_2$, observed great persistence in the pattern of spatial variability in different periods, indicating that areas with higher emissions during the morning had the highest emissions in the afternoon.

## 4. Conclusion

$FCO_2$ showed low spatial-temporal uncertainty coupled with high local-temporal uncertainty estimates. These procedures of uncertainty evaluation allow the identification and characterization of areas susceptible to high emission values. These areas are persistent or not on time or, for example, are influenced by the management of agricultural areas, relief or other soil properties. Thus some measures, such as sample design using denser sampling in regions with the greatest temporal uncertainty, can be adopted to decrease the uncertainty and increase the accuracy in the estimates. However, further studies are needed to establish reference values for the $FCO_2$ and other important greenhouse gases in agricultural soils. The combination of local and spatial uncertainty in different periods for the temporal assessment of these phenomena, a technique proposed in this paper, represents an important tool not yet discussed in the literature. These temporal data can be used in various areas, such as the identification of areas with high yields of crops, areas susceptible to intense rainfall and temperature, and agricultural pest management. This information will also be useful for the determination of specific types of management in each tested environment.

## References


Boix-Fayos, C., Vente, J., Albaladejo, J., Martínez-Mena, M., 2009. Soil carbon erosion and stock as affected by land use changes at the catchment scale in Mediterranean ecosystems. Agr. Ecosyst. Environ. 133, 75–85.

Brito, L.F., Marques, J., Pereira, G.T., La Scala, N., 2010. Spatial variability of soil $CO_2$ emission in different topographic positions. Bragantia 69, 19–27.

Brito, L.F., Marques, J., Pereira, G.T., Souza, Z.M., 2009. Soil $CO_2$ emission of sugar cane fields as affected by topography. Sci. Agric. 66, 77–83.

Cambardella, C.A., Moorman, T.B., Novak, J.M., Parkin, T.B., Karlen, D.L., Turco, R.F., Konopka, A.E., 1994. Field-scale variability of soil properties in central Iowa soils. Soil Sci. Soc. Am. J. 58, 1501–1511.

Cerri, C.C., Galdos, M.V., Maia, S.M.F., Bernoux, M., Feigl, B.J., Powlson, D., Cerri, C.E.P., 2011. Effect of sugar cane harvesting systems on soil carbon stocks in Brazil: an examination of existing data. Eur. J. Soil Sci. 62, 23–28.

Delbari, M., Afrasiab, P., Loiskandl, W., 2009. Using sequential Gaussian simulation to assess the field-scale spatial uncertainty of soil water content. Catena 79, 163–169.

Deutsch, C.V., Journel, A.G., 1998. GSLIB: Geostatistical Software Library: And User's Guide, second ed. Oxford University Press, New York.

Goovaerts, P., 1999. Geostatistics in soil science: state-of-the-art and perspectives. Geoderma 89, 1–45.

Goovaerts, P., 2001. Geostatistical modeling of uncertainty in soil science. Geoderma 103, 3–26.

Grunwald, S., Reddy, K.R., Prenger, J.P., Fisher, M.M., 2007. Modeling of the spatial variability of biogeochemical soil properties in a freshwater ecosystem. Ecol. Model. 201, 521–535.

Herbst, M., Prolingheuer, N., Graf, A., Huisman, J.A., Weihermüller, L., Vanderborght, J., Vereecken, H., 2010. Multivariate conditional stochastic simulation of soil heterotrophic respiration at plot scale. Geoderma 160, 74–82.

Herbst, M., Prolingheuer, N., Graf, A., Huisman, J.A., Weihermüller, L., Vanderborght, J., 2009. Characterization and understanding of bare soil respiration spatial variability at plot scale. Vadose Zone J. 8, 762–771.

IPCC, 2007. Intergovernmental Panel on Climate Change, Climate Change 2007: The Physical Science Basis. Summary for Policymakers. IPCC, Geneva, Switzerland, Available in <http://www.ipcc.ch/publications_and_data/publications_ipcc_fourth_assessment_report_wg1_report_the_physical_science_basis.htm, > (accessed 03.11.11).

Iqbal, J., Hu, R., Feng, M., Lin, S., Malghani, S., Ali, I.M., 2010. Microbial biomass, and dissolved organic carbon and nitrogen strongly affect soil respiration in different land uses: a case study at Three Gorges Reservoir Area, South China. Agr. Ecosyst. Environ. 137, 294–307.

Isaaks, E.H., Srivastava, R.M., 1989. Applied Geostatistics. Oxford University Press, New York.

Juang, K.W., Chen, Y.S., Lee, D.Y., 2004. Using sequential indicator simulation to assess the uncertainty of delineating heavy-metal contaminated soils. Environ. Pollut. 127, 229–238.

Jurasinski, G., Jordan, A., Glatzel, S., 2012. Mapping soil $CO_2$ efflux in an old-growth forest using regression kriging with estimated fine root biomass as ancillary data. Forest Ecol. Manage. 263, 101–113.

La Scala, N., Marques, J., Pereira, G.T., Corá, J.E., 2000. Short-term temporal changes in the spatial variability model of $CO_2$ emissions from a Brazilian bare soil. Soil Biol. Biochem. 32, 1459–1462.

Luan, J., Liua, S., Zhu, X., Wang, J., Liu, K., 2012. Roles of biotic and abiotic variables in determining spatial variation of soil respiration in secondary oak and planted pine forests. Soil Biol. Biochem. 44, 143–150.

Mchunu, C., Chaplot, V., 2012. Land degradation impact on soil carbon losses through water erosion and $CO_2$ emissions. Geoderma 177–178, 72–79.

Morell, F.J., Alvaro-Fuentes, J., Lampurlanés, J., Cantero-Martinez, C., 2010. Soil $CO_2$ fluxes following tillage and rainfall events in a semiarid Mediterranean agroecosystem: effects of tillage systems and nitrogen fertilization. Agr. Ecosyst. Environ. 139, 167–173.

Panosso, A.R., Marques, J., Milori, D.M.B.P., Ferraudo, A.S., Barbieri, D.M., Pereira, G.T., La Scala, N., 2011. Soil $CO_2$ emission and its relation to soil properties in sugar cane areas under Slash-and-burn and Green harvest. Soil Till. Res. 111, 190–196.

Panosso, A.R., Marques, J., Pereira, G.T., La Scala, N., 2009. Spatial and temporal variability of soil $CO_2$ emission in a sugar cane area under green and slash-and-burn managements. Soil Till. Res. 105, 275–282.

Parkin, T.B., 1993. Spatial variability of microbial processes in soil – a review. J. Environ. Qual. 22, 409–417.

Prolingheuer, N., Scharnagl, B., Graf, A., Vereecken, H., Herbst, M., 2010. Spatial and seasonal variability of heterotrophic and autotrophic soil respiration in a winter wheat stand. Biogeosci. Discuss. 7, 9137–9173.

Sugihara, S., Funakawa, S., Kilasara, M., Kosaki, T., 2012. Effects of land management on $CO_2$ flux and soil C stock in two Tanzanian croplands with contrasting soil texture. Soil Biol. Biochem. 46, 1–9.

Teixeira, D.D.B., Panosso, A.R., Cerri, C.E.P., Pereira, G.T., La Scala, N., 2011. Soil $CO_2$ emission estimated by different interpolation techniques. Plant Soil 345, 187–194.

Teixeira, D.D.B., Bicalho, E.S., Panosso, A.R., Perillo, L.I., Iamaguti, J.L., Pereira, G.T., La Scala, N., 2012. Uncertainties in the prediction of spatial variability of soil $CO_2$ emissions and related properties. Rev. Bras. Cienc. Solo 36, 1466–1475.

Zhao, Y., Xu, X., Darilek, J.L., Huang, B., Sun, W., Shi, X., 2009. Spatial variability assessment of soil nutrients in an intense agricultural area, a case study of Rugao County in Yangtze River Delta Region, China. Environ. Geol. 57, 1089–1102.